ACS APPLIED MATERIALS & INTERFACES

Letter

www.acsami.org

Selective Passivation of GeO_2/Ge Interface Defects in Atomic Layer Deposited High-*k* MOS Structures

Liangliang Zhang,[†,‡] Huanglong Li,[†,§,⊥] Yuzheng Guo,[§] Kechao Tang,[∥] Joseph Woicik,[#] John Robertson,[§] and Paul C. McIntyre*[,∥]

[‡]Department of Electrical Engineering, [∥]Department of Materials Science and Engineering, Stanford University, Stanford, California 94305, United States

[§]Engineering Department, Cambridge University, Cambridge CB2 1PZ, United Kingdom

[#]Materials Science and Engineering Laboratory, National Institute of Standards and Technology, Gaithersburg, Maryland 20899, United States

[⊥]Department of Precision Instrument, Tsinghua University, Beijing, China

ABSTRACT: Effective passivation of interface defects in high-k metal oxide/Ge gate stacks is a longstanding goal of research on germanium metal-oxide-semiconductor devices. In this paper, we use photoelectron spectroscopy to probe the formation of a GeO_2 interface layer between an atomic layer deposited Al_2O_3 gate dielectric and a Ge(100) substrate during forming gas anneal (FGA). Capacitance- and conductance-voltage data were used to extract the interface trap density energy distribution. These results show selective passivation of interface traps with energies in the top half of the Ge band gap under annealing conditions that produce GeO_2 interface layer growth. First-principles modeling of Ge/GeO_2 and Ge/GeO/GeO_2 structures and calculations of the resulting partial density of states (PDOS) are in good agreement with the experiment results.

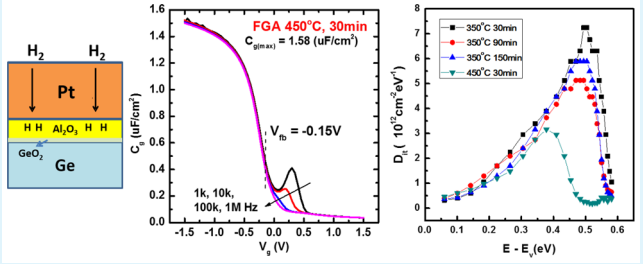

KEYWORDS: *Al_2O_3, Ge, high-k, interface traps, first-principles modeling*

Germanium has been long considered a potential material to replace silicon in future metal-oxide-semiconductor (MOS) devices because of its high intrinsic electron and hole mobilities.[1] The possibility of integrating high-*k* dielectric gate insulators on Ge substrates has been demonstrated,[2,3] leading to numerous subsequent efforts to passivate interface defects in high-*k*/Ge MOS structures, including Si-passivation, nitridation, fluorine passivation, sulfur treatment, etc.[4,5] The GeO_2/Ge MOS system was originally considered problematic compared to SiO_2/Si because of the water solubility and relative thermal instability of GeO_2.[6,7] However, promising results on interface traps were obtained after thermal growth of relatively thick GeO_2 layers on Ge substrate in high pressure oxygen or ozone ambient, achieving interface trap densities (D_{it}) at the 1×10^{11} eV^{-1} cm^{-2} level.[8−11] Theoretical calculations showed that the Ge dangling bond densities at GeO_2/Ge interface are consistent with these low D_{it} values and comparable to values for SiO_2/Si. They result from the low viscosity of GeO_2 at the low temperatures (<600 °C) typically used in Ge MOS device fabrication.[12]

The need to achieve both low D_{it} and low equivalent oxide thickness (EOT) simultaneously, for continued dimensional scaling of field effect devices, prompts research into dielectric processing approaches that form ultrathin GeO_2-like interface layers between high-k dielectrics and the underlying Ge channel. Postmetal gate forming gas (H_2/N_2) anneals (FGA) of atomic layer deposited (ALD)-HfO_2 and ALD-Al_2O_3 dielectrics have been observed to significantly reduce the interface state density of (100) Ge MOS capacitors, and this coincides with an increase in Ge^{4+} bonding at the interface, as detected in synchrotron photoelectron spectroscopy (PES) studies for samples without a gate metal in place.[13,14] Previous reports indicate that the characteristics of the interface defects are strongly influenced by the oxidizing species, such as atomic oxygen, ozone or molecular oxygen.[15−17] It can be inferred from these results that oxidation of the underlying Ge (100) substrate surface during hydrogen-based annealing of ALD-grown Al_2O_3 dielectrics differs from direct oxidation of Ge. This prompts interest in developing a detailed understanding of the relevant defect passivation mechanisms. Interfacial germanium oxide formation during hydrogen anneals may be promoted by residual hydroxyl groups present in the ALD-grown gate dielectric layers, while, for example, in an alternative approach,[18,19] plasma oxidation through an interposed ALD-Al_2O_3 layer is used to produce an ultrathin GeO_X interface layer, followed by deposition of ALD-HfO_2 and metal gate

Received: July 7, 2015
Accepted: September 3, 2015
Published: September 3, 2015

DOI: 10.1021/acsami.5b06087
ACS Appl. Mater. Interfaces 2015, 7, 20499−20506

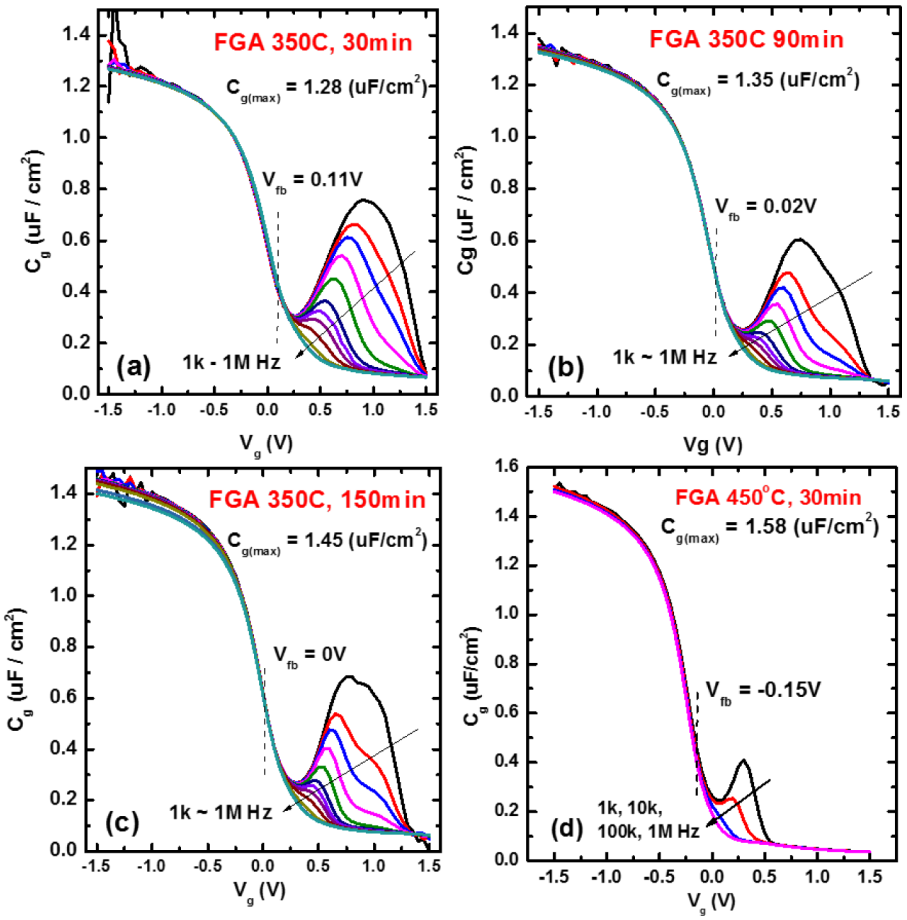

Figure 1. C_g−V_g characteristic of Pt/Al_2O_3/pGe MOSCAPs for different FGA conditions. (a) 350 °C, 30 min; (b) 350 °C, 90 min; (c) 350 °C, 150 min; (d) 450 °C, 30 min.

formation, with no hydrogen anneal used in the gate stack fabrication process. In both processes, growth of a GeO_x layer is found to coincide with a reduction in D_{it}.

In this paper, we present high-energy XPS data demonstrating that hydrogen annealing generates GeO_2 at the interface between ALD-Al_2O_3 and Ge (100) in the presence of a Pt gate electrode. We further show that this GeO_2 layer growth is correlated with the selective reduction of D_{it} at energies in the top half of the Ge band gap. Density functional theory simulations predict the formation of electron traps in this energy range as a result of oxygen deficiency at the germanium oxide/germanium interface.

Pt/Al_2O_3/Ge p-type MOSCAPs are fabricated for capacitance−voltage (CV) characterization. Boron doped p-type Ge (100) substrates (0.2 ohm/square) were rinsed in DI water for about 5 min to remove the water-soluble native oxide and then quickly transferred into the load-lock chamber of an ALD system. The base pressure of the ALD chamber is $\sim 1 \times 10^{-7}$ Torr and the chamber pressure during the ALD process is 0.66 Torr. The thickness of the ALD-grown Al_2O_3 films was measured by ellipsometry, which was calibrated by cross-sectional TEM. Uniform film deposition on 4 in. diameter Si test wafers was confirmed, with <3 Å thickness variation measured by ellipsometry when the film thickness is less than 5 nm. Fifty cycles of H_2O(g) prepulsing[20] was performed prior to Al_2O_3 deposition to functionalize the Ge substrate with hydroxyls (−OH) for better nucleation during the initial ALD cycles. A trimethyl aluminum (TMA)/H_2O cyclic ALD process was performed at a substrate temperature of 170 °C for 35 cycles of Al_2O_3 deposition. The ALD process exhibits excellent linearity of the film thickness with ALD cycle number, and the growth per cycle of the TMA/H_2O process is unaffected by increasing the TMA pulsing time beyond the value of 3 s used in these experiments, indicating that the process is within the ALD window. An average growth rate of 0.75 Å per TMA/H_2O cycle was confirmed by ellipsometry, giving a nominal Al_2O_3 thickness of ∼2.6 nm. A Pt gate electrode of 70 nm thickness was formed by e-beam evaporation through shadow mask with deposition rate 2 Å/s. The back side contact was 15 nm Ti/50 nm Al bilayer metallization. The fabrication is similar to the process used in[21] except that a Fujikin precursor delivery system capable of more accurate control of TMA and H_2O (g) dosing into the chamber was used in this work. (Certain commercial equipment, instruments, or materials are identified in this document. Such identification does not imply recommendation or endorsement by the National Institute of Standards and Technology, nor does it imply that the products identified are necessarily the best available for the purpose.) A high purity forming gas anneal (5% H_2/95% N_2) was performed in a quartz tube furnace after Pt gate deposition. Measurements using a yttria-stabilized zirconia galvanic oxygen sensor indicate that the forming gas ambient produces an oxygen partial pressure (P_{O2}) of $\sim 10^{-24}$ atm in the annealing furnace. Capacitance−voltage (C−V) curves were measured with a HP4284A LCR

DOI: 10.1021/acsami.5b06087
ACS Appl. Mater. Interfaces 2015, 7, 20499−20506

meter at frequencies ranging from 1 kHz to 1 MHz, at room temperature.

Figure 1 shows multifrequency (1 kHz to 1 MHz) $C-V$ characteristics of a typical Pt/Al_2O_3/pGe MOS capacitor with ~2.6 nm Al_2O_3 and different FGA conditions: 350 °C/30 min (Figure 1a), 350 °C/90 min (Figure 1b), 350 °C/150 min (Figure 1c), and 450 °C/30 min (Figure 1d). $C-V$ curves of as-grown samples (without FGA) are not plotted in the figure because they have a very large D_{it} and, as a result, the $C-V$ curves are highly distorted. Among the four $C-V$ curves in Figure 1, there is almost no frequency dispersion from depletion into accumulation, indicating that FGA leads to effective passivation of interface traps with energies lying near to the Ge valence band. The dispersive features in the $C-V$ curves in Figure 1a–d, observed at gate biases, V_g, greater than the flat band voltage (V_{fb}), are caused by trapping and detrapping of electrons and/or holes at traps with energies between approximately midgap and the Ge conduction band edge, corresponding to weak and strong inversion of the Ge substrate. It is observed that the D_{it} features decrease in magnitude from Figure 1a to1b, suggesting that longer FGA at 350 °C is helpful for D_{it} passivation. The Al_2O_3 film is densified during FGA, as indicated by the increasing maximum capacitance $C_{g(max)}$ from Figure 1a to 1c. D_{it} at higher energies in the band gap is slightly increased from Figure 1b to 1c, whereas D_{it} below midgap decreases. These subtle changes in D_{it} distribution suggest slow evolution of trap populations with time during 350 °C FGA, although the detailed mechanisms require further study. FGA at the higher temperature of 450 °C is more helpful for D_{it} passivation, as indicated by the much-reduced false inversion feature in Figure 1d. Further densification of Al_2O_3 and a slight shift of V_{fb} also occur during 450 °C FGA.

To quantify the interface state densities for Pt/Al_2O_3/Ge MOS capacitors annealed under varying FGA conditions (Figure 1), D_{it} versus energy profiles were extracted from multifrequency $C-V$ and conductance-voltage data using the full interface state model.[22,23] All samples exhibit a trend of increasing D_{it} with energy in the Ge gap, with D_{it} less than 1×10^{12} cm^{-2} eV^{-1} near the valence band edge, which agrees well with a qualitative analysis of the $C-V$ characteristics. The curves for all three FGA conditions at 350 °C have a D_{it} peak near the conduction band edge, and the peak value decreases from $\sim 7.5 \times 10^{12}$ cm^{-2} eV^{-1} after 30 min FGA to 5.2×10^{12} cm^{-2} eV^{-1} after 90 min. The D_{it} distributions are similar for the 350 °C/90 and 150 min samples, suggesting that the effect of FGA saturates after ~90 min at 350 °C. The D_{it} near the conduction band is, however, greatly reduced after FGA at 450 °C, leaving a D_{it} peak near midgap, which has similar value ($\sim 3 \times 10^{12}$ cm^{-2} eV^{-1}). The D_{it} for energies in the bottom half of the band gap is comparable for all the FGA conditions represented in Figures 1 and 2. In comparison to the D_{it} distribution observed in this study, relatively symmetric, U-shaped distributions were reported for the direct oxidation of Ge (100) wafers using various oxidant species,[15,16] except in the case where atomic oxygen, a very active oxidant, was used.[13] This difference indicates the distinct nature of the interface defect population produced by subcutaneous oxidation during forming gas annealing of ALD-Al_2O_3 coated Ge (100).

To better understand the chemical states of germanium in the ALD-Al_2O_3/Ge interface region, soft X-ray synchrotron PES at the Stanford Synchrotron Radiation Laboratory (SSRL) Beamline 8–1 is used. Synchrotron light is directed into an ultrahigh vacuum (UHV) chamber with pressure maintained at 5×10^{-11} Torr, and the photoelectrons are collected by an electron energy analyzer. The pass energy is set to 23 eV, which provides a detector energy resolution of 0.1 eV. The incoming photon energy is 120 eV, giving the emitted Ge 3d core electrons an electron mean free path of approximately 1 nm. This technique is very surface sensitive and ideal for differentiating Ge +1, +2, +3, +4 components producing the chemical shift of Ge 3d oxide peak (bonding energy near 29 eV).[7] A 1.1 nm thickness Al_2O_3 layer was grown on Ge by ALD for PES analysis. The selected Al_2O_3 thickness is thinner than that tested electrically due to the limited detection depth of the 120 eV photons. To determine the surface roughness, we randomly selected multiple 2 μm × 2 μm areas on the film for noncontact AFM imaging using a Park Systems XE-70. The measured root-mean-square (RMS) roughness is around 0.23 nm, less than the nominal thickness of Al_2O_3 (1.1 nm), suggesting that the Al_2O_3 films are effectively pinhole free.

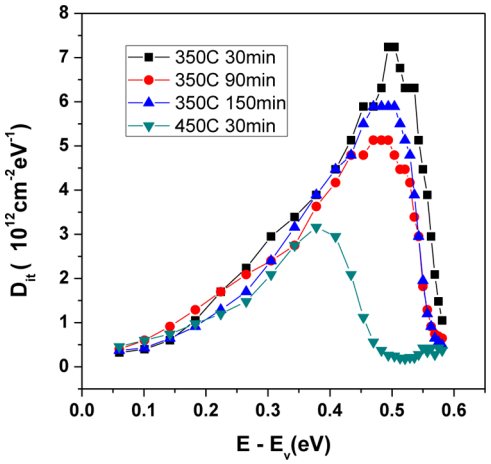

Figure 2. D_{it} extracted using the full interface state model[8,9] for different FGA conditions.

The Ge 3d and corresponding GeO_x peaks of samples treated with various FGA conditions are shown in Figure 3. Spin–orbit splitting of the Ge $3d_{1/2}$ and $3d_{3/2}$ peaks is clearly observed, indicating good energy resolution of the measurement. The as-grown Al_2O_3/Ge sample without any FGA treatment exhibits a small tail of GeO_x, consistent with nearly complete removal of native germanium oxide during the DI water clean and almost no regrowth of Ge oxide during ALD deposition, leaving very little GeO_x on the as-grown sample. After FGA at 350 °C for 30 min, the spectrum of GeO_x is best fitted by a mixture of Ge +1, +2, +3, and +4 peaks, indicating a GeO_x layer at Al_2O_3/Ge interface. These results, that passivation of high-k/Ge interface defects coincides with formation of a thin GeO_x layer between the ALD high-k layer and a Ge channel, are consistent with findings in references 8 and 12. The $C-V$ curves are greatly improved in terms of frequency dispersion and the D_{it} feature after FGA at 350 °C for 30 min. Comparing Figure 3b to Figure 3c, the FGA temperature is kept at 350 °C, and the anneal time is increased from 30 to 60 min. An increase of the chemically shifted Ge +4 peak is observed for increasing FGA time, suggesting more GeO_2 is formed between Al_2O_3 and Ge. After increasing the FGA temperature to 400 °C, the Ge +4 peak intensity is further increased, and the spectrum is best fitted by only Ge +3 and +4 peaks, without any Ge +1 and +2 features.

DOI: 10.1021/acsami.5b06087
ACS Appl. Mater. Interfaces 2015, 7, 20499–20506

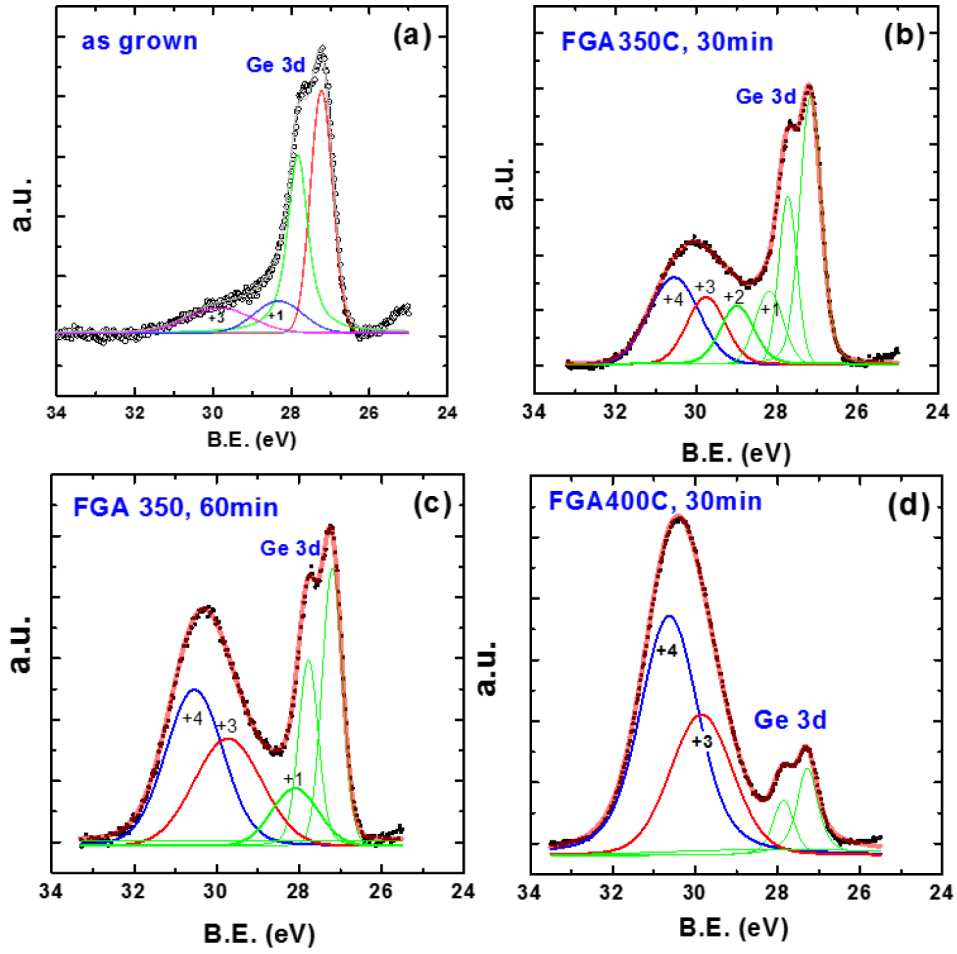

Figure 3. (a–d) Ge 3d and GeO_x peak measured by PES at SSRL Beamline 8–1 with photon energy of 120 eV.

The above analysis leads to the following model that, during FGA, hydrogen may diffuse to the Al_2O_3/Ge interface and react with residual hydroxyls incorporated during growth of the ALD-Al_2O_3, producing H_2O. The water molecules thus formed can further react with Ge and GeO to form GeO_2. This proposed reaction is consistent with prior experiments on high-k oxides on Ge substrates.[13,14] Furthermore, the very low P_{O2} measured for the FGA atmosphere in these experiments, $\sim 10^{-24}$ atm, does not permit direct oxidation of the Ge to GeO_2 without an additional oxidant such as residual OH groups/H_2O.

The soft X-ray PES spectra shown in the previous section has the fine energy resolution and surface sensitivity to readily decompose different chemical states of elements in the gate oxide/interface region. However, this ultrahigh surface sensitivity sacrifices the probing depth (~1 nm for photoelectrons excited by 120 eV photons). The Ge-MOS capacitors studied by electrical testing in this work has a Pt/Al_2O_3/Ge structure in which the oxide/Ge interface is covered by layers that are much thicker than 1 nm. The Pt gate also helps to dissociate H_2 to atomic H, which may contribute to the reaction with −OH group in the ALD-Al_2O_3 and, therefore, to GeO_2 formation. As a result, for PES analysis, it is important to include a gate metal layer on Al_2O_3/Ge to simulate gate stacks under FGA conditions.

Hard X-ray synchrotron PES (HAXPES) is suitable for these measurements because of the greater collection depth of bonding information resulting from the relatively high incident photon energies. Data were recorded at the National Institute of Standards and Technology Beamline x-24A, which is equipped with a Si(111) double-crystal monochromator and a hemispherical electron analyzer that select photons with energies ranging from 2 to 5 keV. Details of the beamline and vacuum system have been reported previously.[24] In this experiment, a photon energy of 4150 eV was chosen to permit probing at depths more than 10 nm below the surface of our samples. The pass energy of the electron energy analyzer was set to 200 eV, which provides an energy resolution around 0.5 eV. To account for small energy shifts of the incident photon beam, which can occur during long measurement times, the 3d peak and Fermi edge of a silver thin film were both measured before and after each sample was characterized, to provide a reference. The samples are prepared by the same process as we used to fabricate MOS capacitors. The Al_2O_3 layer is produced using 25 TMA/H_2O cycles (1.9 nm nominal thickness) and the thickness of the Pt gate is 8 nm. Samples without FGA treatment (as-grown), with FGA at 350 °C for 30 min, and with FGA at 450 °C for 30 min were characterized, and the measured spectra are shown in Figure 4. The spectra are normalized using their Ge 2p peak substrate intensities, and vertically shifted for better display. There is no GeO_x signal detected by HAXPES on the as-grown sample, and there is a germanium oxide tail observed for the sample prepared with FGA at 350 °C for 30 min, suggesting that the Al_2O_3/Ge interface is coated by a very thin GeO_x layer. After 450 °C, 30 min FGA, the germanium oxide is more obvious, and is mostly

DOI: 10.1021/acsami.5b06087
ACS Appl. Mater. Interfaces 2015, 7, 20499–20506

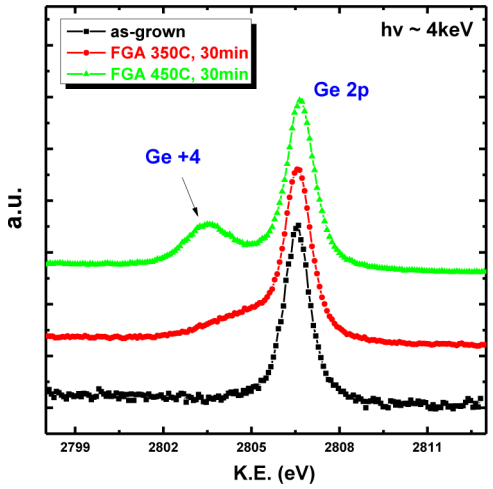

Figure 4. Ge 2p and GeO_x peak measured by hard X-ray synchrotron PES at NSLS beamline x24-a with photon energy of 4 keV.

GeO_2 according to the energy shift of Ge oxide peak relative to the Ge 2p substrate peak.[25] These results are in agreement with our analysis in previous parts of this paper.

To determine the interface bonding configuration between Ge and an overlying suboxide or oxide layer, first-principles modeling is performed. The interface region is modeled in a supercell including 15 Å vacuum layer to separate the slab in the direction normal to the interface. Dangling bonds on each side of the slab are terminated by hydrogen atoms. Thick Ge slab (10 layers) is used. Various bonding geometries are modeled on a 2 × 2 reconstruction of Ge surfaces. The CASTEP plane wave density functional code[26,27] is used for total energy and electronic structure calculation. The exchange-correlation of electrons is presented by the generalized gradient approximation (GGA).[28] Ultrasoft pseudopotentials with 380 eV cutoff energy and 2 × 2 × 1 Monkhorst–Pack k point sampling scheme are used for structural relaxation. In order to remedy the band gap underestimation problem of GGA, screened exchange hybrid functional (sX)[29] is applied on the GGA relaxed structure to calculate the partial density of states (PDOSs) across the interface. Norm-conserving pseudopotentials with 680 eV cutoff energy are used for sX calculation. Details of the calculation can be found in ref 30. Previous DFT calculations[31−37] have studied defects in bulk GeO_2 and simple oxygen vacancy defects at the interface.[12] Here we consider the defects and possible anomalous bonding configurations at the Ge/GeO_2 interface.

There are three possible types of defects at a Ge/GeO_2 interface.[31−37] The first is a Ge dangling bond on the Ge side, or P_b center. The second is an interfacial O vacancy. This leaves two Ge dangling bonds, which can rebond to form a single Ge–Ge bond just inside the GeO_2. The third consists of a rearrangement of the Ge–Ge bond where one Ge relaxes backward and binds to an O behind, retaining the 4-fold configuration (referred to as 4-fold Ge defect). This leaves a so-called valence alternation pair (VAP) defect[38,39] which consists of a 3-fold bonded Ge^- site near a 3-fold bonded O^+ site (VAP with a 4-fold Ge defect is referred to as Ge4-VAP), and is similar to that previously considered by Binder.[33] The charges indicated are formal ionic charges which create an overall closed electronic shell.

The Ge dangling bond gives rise to a state just at the valence band (VB) edge,[32] which is half-filled when neutral. The reconstructed Ge–Ge bond gives rise to states which would lie deep in the Ge VB, and well into the Ge conduction band (CB), respectively. Considering the forgoing experimental data (Figures 1 and 2), the VAP is interesting as it gives rise to two defect states that lie close to the Ge band edges. One filled state is on the 3-fold Ge site, with energy level near the VB edge. The other empty state associates with the 4-fold Ge site, and its energy level lies near the CB edge.[33,34] These states can be seen in the supercell calculations of Figure 5.

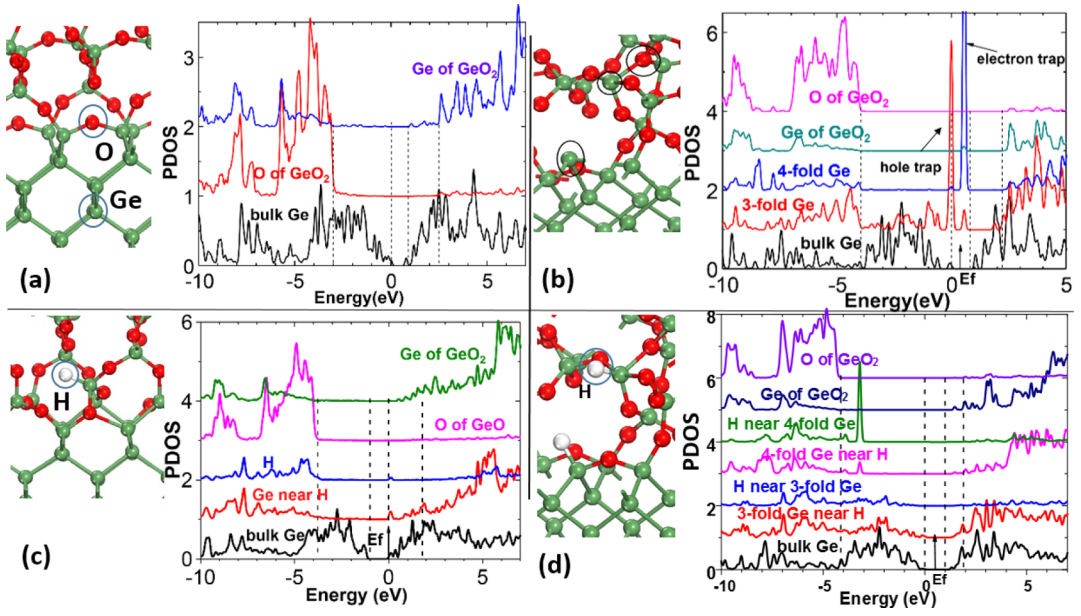

Figure 5. (a) Atomic structure and PDOS of defect-free Ge/GeO_2. (b) Atomic structure and PDOS of the Ge/GeO_2 interface with VAP defects. At the VAP, the electron trap orbital is localized on the Ge sites adjacent to the 3-fold oxygen site. (c) Hydrogen passivation of the Ge 3-fold defect site by forming a Ge–H bond, and removal of states from band gap. (d) Hydrogen passivation of both the 3-fold Ge defect site and the 4-fold Ge defect site leads to the formation of a 4-fold Ge and a 5-fold Ge, respectively, both with a Ge–H bond, and removal of states from the band gap.

DOI: 10.1021/acsami.5b06087
ACS Appl. Mater. Interfaces 2015, 7, 20499–20506

Figure 5a shows the defect-free Ge/GeO_2 interface with the 4-fold interfacial Ge and 2-fold O sites, and the corresponding PDOS. It has a clean Ge band gap without any defect states. We start the simulation of VAP defects with a $Ge/GeO/GeO_2$ structure, which simulates an unannealed structure that has a combination of GeO and GeO_2 near the interface (data not shown). Defects such as VAP dipoles are then intentionally introduced in the structure. Figure 5b shows the atomic structure and PDOS of a Ge/GeO_2 interface with a Ge4-VAP whose dipoles points toward the interface with Ge. It is different from GeO-like VAP defects, in that the 3-fold O bonded is detached from 3-fold Ge. 3-fold Ge and 4-fold Ge in (b) both form partial defects states within the Ge band gap, where defect states from the 3-fold Ge has a larger peak closer to valence band maximum and a smaller peak closer conduction band minimum, while that from the 4-fold Ge is closer to the conduction band minimum. It is found from the modeling that Ge/GeO_2 has a defect free interface within the Ge band gap, while $Ge/GeO/GeO_2$ structure can have a large density of defect states near the valence band, and introducing VAP dipoles in Ge/GeO_2 interface can lead to defects with energies close to both the valence and conduction band edges. The large density of defect states in the $Ge/GeO/GeO_2$ structure agree well with existing literature reports that GeO will cause O deficiency defects with energy levels near the valence band edge.[16,40]

We also calculated here the effect of hydrogen atoms interacting with these defects. Hydrogen has the effect of removing both the electron and hole traps from the band gap energy range. In passivation of the GeO-like interfacial VAP, atomic hydrogen adds to the 3-fold Ge site, to form a Ge−H bond, removing the hole trap from the gap and passivating this site, as shown in Figure 5c. This occurs with little energy barrier. In passivation of the Ge4-VAP, two hydrogen atoms sit on the 3-fold Ge site and 4-fold Ge defect site, respectively. This leaves a 4-fold and a 5-fold Ge site, both without any gap state, which is illustrated in Figure 5d. We also note that there is a localized state on the H near 4-fold Ge with energy level deep in the Ge band gap, which is quite nonbonding. This results from a multicenter orbital interaction, similar to the $Si(5)H^-$ configuration in its SiO_2 counterpart.[41] It is possible for the hydrogen atom to insert into the 4-fold Ge and 3-fold O bond with an energy barrier, and break it, leaving normal 4-fold Ge and 2-fold O sites. Thus, H can passivate the electron trap state as well as the hole trap; however, these reactions occur with a greater energy barrier for passivation of the electron trap associated with the 4-fold Ge defect.

These observations are consistent with our experimental results. Low temperature (≤350 °C) forming gas anneals performed for 30 min in these experiments significantly reduce the interface trap density across the band gap compared to the unannealed case, although the resulting D_{it} distribution is asymmetric. As depicted in Figure 2, the interface trap density is greatest near the CB edge and this is consistent with the greater predicted energy barrier for H passivation of 4-fold Ge electron traps at the GeO_x/Ge interface. With increasing FGA temperature and annealing time, PES spectra show that the oxide interlayer nonstoichiometry is reduced, producing more GeO_2-like bonding. This should correspond to a reduced density of both 3-fold Ge and 4-fold Ge defects near the interface. As the 3-fold Ge hole traps near the VB edge are predicted to be more easily passivated by hydrogen alone, the selective removal of interface traps observed at energies in the top half of the Ge band gap (Figure 2) may result primarily from the improved GeO_x stoichiometry after annealing. However, a contribution from the improved kinetics of H passivation of the 4-fold Ge electron traps cannot be ruled out, for the higher temperature (450 °C) annealed samples.

Second ion mass spectrometry (SIMS) characterization was used to examine the DFT prediction that hydrogen will preferentially bind at defects in the $Al_2O_3/GeO_2/GeO/Ge$ interface region of Pt-gated Ge MOS structures. The characterization is performed with Cameca NanoSIMS 50L which has both high mass resolution and subppm sensitivity, with a lateral spatial resolution down to 50 nm. Samples with and without annealing are analyzed by depth profiling through the overlying Pt gate and into the oxide and substrate. In this experiment, N_2/D_2 (5%) deuterated forming gas was used to anneal a sample at 350 °C for 30 min. Use of D_2 rather than H_2 forming gas makes it possible to distinguish between hydrogen bound to impurity species incorporated in the film during TMA/H_2O ALD and that introduced during the FGA. SIMS depth profiles pre- and post-FGA are shown in Figure 6. The

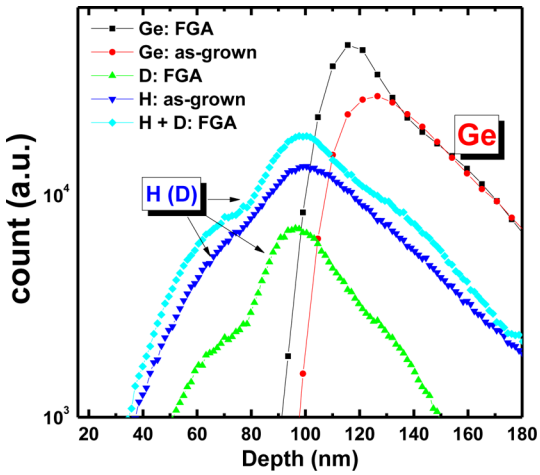

Figure 6. SIMS depth profiles of hydrogen, deuterium, and germanium in $Pt/Al_2O_3/Ge$ MOSCAPs before and after N_2/D_2 anneal.

Ge profiles are included for easier identification of the interface. The summation of the counts of hydrogen and of deuterium (H + D) of the annealed sample is compared to the hydrogen (H) detected in the as-grown sample. The D signal from the as-grown sample is negligible and is not shown. The depth profiles show H and D signals that peak at the oxide/Ge interface. Deuterium is clearly incorporated into the Al_2O_3 film and in the interface region after the anneal, and there is a ∼ 40% increase of H + D in the annealed sample compared to the initial H profile. This indicates that the deuterium FGA produces a net introduction of hydrogen-related species into the Al_2O_3 film and interface region, rather than simply promoting isotope exchange with incorporated hydrogen impurity species.

To summarize, we report selective passivation of interface defects in high-*k* metal oxide/Ge stacks coinciding with interfacial GeO_2 growth that occurs during H_2/N_2 annealing of $Pt/ALD\text{-}Al_2O_3/Ge$ gate stacks. *C*−*V* characteristics and interface trap energy distributions of high-quality $Pt/Al_2O_3/Ge$ MOSCAPs under multiple annealing conditions are investigated in detail, and results suggest reduction of D_{it} between midgap and the Ge conduction band edge after FGA 450 °C.

DOI: 10.1021/acsami.5b06087
ACS Appl. Mater. Interfaces 2015, 7, 20499−20506

Soft and hard X-ray synchrotron PES techniques were used to probe the generation of the Ge +4 chemical state in the gate stack, indicating the generation of GeO_2 interface layer between ALD-Al_2O_3 layer and the Ge substrate. The experimental results agree well with first principle calculations on Ge/GeO/GeO_2 and Ge/GeO_2 structures, in which elimination of GeO-like bonding from the interface removes O deficiency defects near the valence band edge of Ge and VAP dipole defects near the Ge surface that produce defect states closer to the conduction band edge. In addition, the passivation of the 4-fold Ge electron traps by atomic H at elevated temperature is also analyzed by simulation. Finally, SIMS depth profiles support the results of DFT calculation that predict binding of H to the 3-fold Ge defects in the GeO_2/GeO/Ge interface region. This complex interplay of hydrogen defect passivation and redox chemistry leading to interface oxidation may be relevant in other high-k MOS systems.[42]

AUTHOR INFORMATION

Corresponding Author

*E-mail: pcm1@stanford.edu.

Author Contributions

†L.Z. and H.L. contributed equally to this report.

Notes

The authors declare no competing financial interest.

ACKNOWLEDGMENTS

This work was supported in part by the Stanford Initiative for Nanoscale Materials and Processes (INMP). This work was performed at the National Synchrotron Light Source and the Stanford Synchrotron Radiation Laboratory, which are supported by the US Department of Energy. Additional support was provided by the National Institute of Standards and Technology. Part of this work was performed at the Stanford Nano Shared Facilities (SNSF) and Dr. Charles Hitzman helped the nano-SIMS measurement. The authors thank Prof. Piero A. Pianetta and Prof. Krishna Saraswat of Stanford University for useful comments and suggestions. J.R. thanks EPSRC for Funding support.

REFERENCES

(1) Wallace, R. M.; Mcintyre, P. C.; Kim, J.; Nishi, Y. Atomic Layer Deposition Of Dielectrics on Ge and III−V Materials for Ultrahigh Performance Transistors. *MRS Bull.* **2009**, *34*, 493−503.

(2) Chui, C. O.; Kim, H.; Mcintyre, P. C.; Saraswat, K. C. A Germanium NMOSFET Process Integrating Metal Gate and Improved Hi-κ Dielectrics. *IEEE Int. Electron Dev. Mtg. (IEDM) Technol. Dig.* **2003**, 437−440.

(3) Chui, C. O.; Kim, H.; Chi, D.; Triplett, B.; Mcintyre, P. C.; Saraswat, K. C. A Sub-400 °C Germanium MOSFET Technology with High-k Dielectric and Metal Gate. *IEEE Int. Electron Dev. Mtg. (IEDM) Technol. Dig.* **2002**, 437−440.

(4) Xie, Q.; Deng, S.; Schaekers, M.; Lin, D.; Caymax, M.; Delabie, A.; Qu, X.-P.; Jiang, Y.-L.; Deduytsche, D.; Detavernier, C. Germanium Surface Passivation and Atomic Layer Deposition of High-k Dielectrics - a Tutorial Review on Ge-Based MOS Capacitors. *Semicond. Sci. Technol.* **2012**, *27*, 074012−074012.

(5) Bodlaki, D.; Yamamoto, H.; Waldeck, D.; Borguet, E. Ambient Stability of Chemically Passivated Germanium Interfaces. *Surf. Sci.* **2003**, *543*, 63−74.

(6) Brunco, D. P.; De Jaeger, B.; Eneman, G.; Satta, A.; Terzieva, V.; Souriau, L.; Leys, F. E.; Pourtois, G.; Houssa, M.; Opsomer, K.; Nicholas, G.; Meuris, M.; Heyns, M. Germanium: The Past And Possibly a Future Material for Microelectronics. *ECS Trans.* **2007**, 479−493.

(7) Bellenger, F.; Houssa, M.; Delabie, A.; Conard, T.; Caymax, M.; Meuris, M.; Meyer, K. D.; Heyns, M. Electrical Passivation of the (100) Ge Surface by Its Thermal Oxide. *ECS Trans.* **2007**, 451−459.

(8) Delabie, A.; Bellenger, F.; Houssa, M.; Conard, T.; Van Elshocht, S.; Caymax, M.; Heyns, M.; Meuris, M. Effective Electrical Passivation of Ge(100) for High-k Gate Dielectric Layers Using Germanium Oxide. *Appl. Phys. Lett.* **2007**, *91*, 082904.

(9) Kuzum, D.; Pethe, A. J.; Krishnamohan, T.; Oshima, Y.; Sun, Y.; Mcvittie, J. P.; Pianetta, P. A.; Mcintyre, P. C.; Saraswat, K. C. Interface-Engineered Ge (100) And (111), N- and P-FETs with High Mobility. *IEEE Int. Electron Dev. Mtg. (IEDM) Technol. Dig.* **2007**, 723−726.

(10) Lee, C. H.; Tabata, T.; Nishimura, T.; Nagashio, K.; Kita, K.; Toriumi, A. Ge/GeO_2 Interface Control With High-Pressure Oxidation for Improving Electrical Characteristics. *Appl. Phys. Express* **2009**, *2*, 071404.

(11) Kamata, Y.; Takashima, A.; Tezuka, T. Material Properties, Thermal Stabilities And Electrical Characteristics of Ge MOS Devices, Depending on Oxidation States of Ge Oxide: Monoxide [GeO(II)] and Dioxide [GeO_2(IV)]. *MRS Online Proc. Libr.* **2009**, DOI: 10.1557/PROC-1155-C02-04.

(12) Houssa, M.; Pourtois, G.; Caymax, M.; Meuris, M.; Heyns, M. M.; Afanas'Ev, V. V.; Stesmans, A. Ge Dangling Bonds at the (100)Ge/GeO_2 Interface and the Viscoelastic Properties of GeO_2. *Appl. Phys. Lett.* **2008**, *93*, 161909.

(13) Swaminathan, S.; Sun, Y.; Pianetta, P.; Mcintyre, P. C. Ultrathin ALD-Al_2O_3 Layers for Ge (001) Gate Stacks: Local Composition Evolution and Dielectric Properties. *J. Appl. Phys.* **2011**, *110*, 094105−1−6.

(14) Oshima, Y.; Sun, Y.; Kuzum, D.; Sugawara, T.; Saraswat, K. C.; Pianetta, P.; Mcintyre, P. C. Chemical Bonding, Interfaces, And Defects in Hafnium Oxide/Germanium Oxynitride Gate Stacks on Ge(100). *J. Electrochem. Soc.* **2008**, *155*, G304−09.

(15) Baldovino, S.; Lamperti, A.; Fanciulli, M.; Molle, A. Role of the Oxygen Content in the GeO2 Passivation of Ge Substrates as a Function of the Oxidizer. *J. Electrochem. Soc.* **2012**, *159* (6), H555−H559.

(16) Kuzum, D.; Krishnamohan, T.; Pethe, A. J.; Okyay, A. K.; Oshima, Y.; Sun, Y.; Mcvittie, J. P.; Pianetta, P. A.; Mcintyre, P. C.; Saraswat, K. C. Ge-Interface Engineering With Ozone Oxidation For Low Interface-State Density. *IEEE Electron Device Lett.* **2008**, *29*, 328−330.

(17) Baldovino, S.; Molle, A.; Fanciulli, M. Influence Of the Oxidizing Species on the Ge Dangling Bonds at the (100)Ge/GeO_2 Interface. *Appl. Phys. Lett.* **2010**, *96*, 222110.

(18) Zhang, R.; Iwasaki, T.; Taoka, N.; Takenaka, M.; Takagi, S. High-Mobility Ge PMOSFET With 1nm EOT Al_2O_3/GeOx/Ge Gate Stack Fabricated by Plasma Post Oxidation. *IEEE Trans. Electron Devices* **2012**, *59*, 335−341.

(19) Zhang, R.; Huang, P. C.; Taoka, N.; Takenaka, M.; Takagi, S. High Mobility Ge PMOSFETs with 0.7 nm Ultrathin EOT Using HfO_2/Al_2O_3/GeOx/Ge Gate Stacks Fabricated by Plasma Post Oxidation. *VLSI symp.* **2012**, 161−162.

(20) Swaminathan, S.; Oshima, Y.; Kelly, M. A.; Mcintyre, P. C. Oxidant Prepulsing of Ge (100) Prior to Atomic Layer Deposition of Al_2O_3: In Situ Surface Characterization. *Appl. Phys. Lett.* **2009**, *95*, 032907.

(21) Zhang, L.; Gunji, M.; Thombare, S.; Mcintyre, P. C. EOT Scaling Of TiO_2/Al_2O_3 on Germanium PMOSFETs and Impact of Gate Metal Selection. *IEEE Electron Device Lett.* **2014**, *34*, 732−734.

(22) Yuan, Y.; Yu, B.; Ahn, J.; Mcintyre, P. C.; Asbeck, P. M.; Rodwell, M. J. W.; Taur, Y. A Distributed Bulk-Oxide Trap Model For Al_2O_3 InGaAs MOS Devices. *IEEE Trans. Electron Devices* **2012**, *59*, 2100−2106.

(23) Chen, H.-P.; Yuan, Y.; Yu, B.; Ahn, J.; Mcintyre, P. C.; Asbeck, P. M.; Rodwell, M. J. W.; Taur, Y. Interface-State Modeling of Al_2O_3-

DOI: 10.1021/acsami.5b06087
ACS Appl. Mater. Interfaces 2015, 7, 20499−20506

InGaAs MOS From Depletion to Inversion. *IEEE Trans. Electron Devices* **2012**, *59* (9), 2383−2389.
(24) Weiland, C.; Rumaiz, A.; Lysaght, P.; Karlin, B.; Woicik, J.; Fischer, D. NIST High Throughput Variable Kinetic Energy Hard X-Ray Photoelectron Spectroscopy Facility. *J. Electron Spectrosc. Relat. Phenom.* **2013**, *190*, 193−200.
(25) Wang, D.; Chang, Y.-L.; Wang, Q.; Cao, J.; Farmer, D. B.; Gordon, R. G.; Dai, H. Surface Chemistry And Electrical Properties of Germanium Nanowires. *J. Am. Chem. Soc.* **2004**, *126* (37), 11602−11611.
(26) Milman, V.; Winkler, B.; White, J. A.; Pickard, C. J.; Payne, M. C.; Akhmatskaya, E. V.; Nobes, R. H. Electronic Structure, Properties, and Phase Stability of Inorganic Crystals: A Pseudopotential Plane-Wave Study. *Int. J. Quantum Chem.* **2000**, *77*, 895−910.
(27) Segall, M. D.; Lindan, P. J. D.; Probert, M. J.; Pickard, C. J.; Hasnip, P. J.; Clark, S. J.; Payne, M. C. First-Principles Simulation: Ideas, Illustrations and the CASTEP Code. *J. Phys.: Condens. Matter* **2002**, *14*, 2717−2744.
(28) Perdew, J. P.; Burke, K.; Ernzerhof, M. Generalized Gradient Approximation Made Simple. *Phys. Rev. Lett.* **1997**, *78*, 3865−3868.
(29) Bylander, D. M.; Kleinman, L. Good Semiconductor Band Gaps with a Modified Local-Density Approximation. *Phys. Rev. B: Condens. Matter Mater. Phys.* **1990**, *41*, 7868−7871.
(30) Li, H. First Principle Modeling of High-K Oxide on Ge. *PhD thesis*, University of Cambridge, Cambridge, U.K., 2014.
(31) Weber, J. R.; Janotti, A.; Rinke, P.; Van de Walle, C. G. Dangling-Bond Defects and Hydrogen Passivation in Germanium. *Appl. Phys. Lett.* **2007**, *91*, 142101.
(32) Broqvist, P.; Alkauskas, A.; Pasquarello, A. Defect Levels of Dangling Bonds in Silicon and Germanium through Hybrid Functionals. *Phys. Rev. B: Condens. Matter Mater. Phys.* **2008**, *78*, 075203.
(33) Binder, J. F.; Broqvist, P.; Pasquarello, A. Charge Trapping in Substoichiometric Germanium Oxide. *Microelectron. Eng.* **2011**, *88*, 1428−1431.
(34) Li, H.; Robertson, J. Defects at Ge:GeO_2 and Ge:MeO_x Interfaces. *Microelectron. Eng.* **2013**, *109*, 244−249.
(35) Xiong, K.; Lin, L.; Robertson, J.; Cho, K. Energetics of Hydrogen in GeO_2, Ge, and Their Interfaces. *Appl. Phys. Lett.* **2011**, *99*, 032902.
(36) Li, H.; Lin, L.; Robertson, J. Identifying a Suitable Passivation Route for Ge Interfaces. *Appl. Phys. Lett.* **2012**, *101*, 052903.
(37) Binder, J. F.; Broqvist, P.; Komsa, H.-P.; Pasquarello, A. Germanium Core-Level Shifts at Ge/GeO_2 Interfaces through Hybrid Functionals. *Phys. Rev. B: Condens. Matter Mater. Phys.* **2012**, *85*, 245305.
(38) Kastner, M.; Adler, D.; Fritzsche, H. Valence-Alternation Model For Localized Gap States in Lone-Pair Semiconductors. *Phys. Rev. Lett.* **1976**, *37*, 1504.
(39) O'Reilly, E. P.; Robertson, J. Theory of Defects in Vitreous Silicon Dioxide. *Phys. Rev. B: Condens. Matter Mater. Phys.* **1983**, *27*, 3780−3795.
(40) Matsubara, H.; Sasada, T.; Takenaka, M.; Takagi, S. Evidence of Low Interface Trap Density in GeO_2/Ge Metal-Oxide-Semiconductor Structures Fabricated by Thermal Oxidation. *Appl. Phys. Lett.* **2008**, *93*, 032104.
(41) Blöchl, P. E. First-Principles Calculations of Defects in Oxygen-Deficient Silica Exposed to Hydrogen. *Phys. Rev. B: Condens. Matter Mater. Phys.* **2000**, *61*, 6158−6179.
(42) Zhang, K.; Kim, S. J.; Zhang, Y.; Heeg, T.; Schlom, D. G.; Shen, W.; Pan, X. Epitaxial Growth of ZnO on (1 1 1) Si Free of an Amorphous Interlayer. *J. Phys. D: Appl. Phys.* **2014**, *47*, 105302.

DOI: 10.1021/acsami.5b06087
ACS Appl. Mater. Interfaces 2015, 7, 20499−20506